Original Investigation

Second-order Texture Measurements of ^{3}He Ventilation MRI: Proof-of-concept Evaluation of Asthma Bronchodilator Response

Nanxi Zha, BEng[1], Damien Pike, BSc[1], Sarah Svenningsen, BMSc[1], Dante P. I. Capaldi, BSc[1], David G. McCormack, MD FRCPC[2], Grace Parraga, PhD[1]

Rationale and Objectives: ^{3}He magnetic resonance imaging (MRI) can be used to quantify functional responses to asthma therapy and provocation. Ventilation imaging offers quantitative information beyond ventilation defects that have not yet been exploited. Therefore, our objective was to evaluate hyperpolarized ^{3}He MRI ventilation defect percent (VDP) and compare this and pulmonary function measurements to ventilation image texture features and their changes post-bronchodilator administration in patients with asthma.

Materials and Methods: Volunteers with a diagnosis of asthma provided written informed consent to an ethics board-approved protocol and underwent pulmonary function tests and MRI before and after salbutamol inhalation. MR images were analyzed using VDP, and their texture was evaluated via gray-level run-length matrices. These texture classifiers were compared to VDP in responders to bronchodilation based on VDP (VDP responders) and forced expiratory volume in 1 s (FEV_1) (FEV_1 responders).

Results: In total, 47 patients with asthma (18 males 39 ± 13 years, FEV_1 = 79 ± 21%) reported significantly improved FEV_1, FEV_1/forced vital capacity (FVC), residual volume (RV)/total lung capacity (TLC) (all P = .0001) and VDP (P = .01) post-salbutamol. Post-salbutamol, VDP responders and nonresponders to salbutamol were significantly different for coarse-texture features including long-run emphasis (LRE) and long-run, low gray-level emphasis (LRLGE, both P < .05) and for FEV_1 responders to salbutamol, there was significantly different long-run, high gray-level emphasis (LRHGE, P = .04). There were significant relationships for VDP with LRE (R = .50, P = .0003), LRLGE (R = .34, P = .02), and LRHGE (R = .56, P = .0001). Receiver operating characteristic curves showed VDP with the strongest performance (AUC = .92), followed by coarse-texture classifier LRHGE (AUC = .83), FEV_1 (AUC = .80), LRE (AUC = .66), FVC (AUC = .58), and LRLGE (AUC = .42).

Conclusions: In patients with asthma, differences in ventilation patchiness post-salbutamol can be quantified using coarse-texture classifiers that are significantly different in bronchodilator responders.

Key Words: Texture analysis; asthma; bronchodilator response; ^{3}He MRI.

INTRODUCTION

Asthma is a chronic inflammatory disease of the small and medium airways caused by smooth muscle hyperresponsiveness and inflammation, leading to intermittent symptoms of dyspnea, coughing, chest tightness, and wheezing (1). Global estimates indicate that approximately 300 million adults and children report an asthma diagnosis, and this is expected to increase in the future (2). Short- and long-acting bronchodilators are commonly administered to ease dyspnea and other symptoms (3), and importantly, the joint American Thoracic Society (ATS)-European Respiratory Society guidelines define a significant bronchodilator response of forced expiratory volume in 1 s (FEV_1) or forced vital capacity (FVC) improvement of 200 mL and 12% or greater respectively, as considered definitive for asthma (4). Bronchodilator response thresholds are controversial, however, because spirometry measurements do not always reflect bronchodilator response in terms of symptomatic relief (5).

Magnetic resonance imaging (MRI) using hyperpolarized noble gases such as ^{3}He and ^{129}Xe (6) provides a way to visualize and

Acad Radiol 2016; 23:176–185

From the Imaging Research Laboratories, Robarts Research Institute, 1151 Richmond Street North, London, ON N6A 5B7, Canada (N.Z., D.P., S.S., D.PI.C., G.P.); Department of Medical Biophysics (D.P., S.S., D.PI.C., G.P.); Division of Respirology, Department of Medicine (D.G.MC.), The University of Western Ontario, London, Canada. Received August 13, 2015; revised September 22, 2015; accepted October 5, 2015. [1]Present address: Imaging Research Laboratories, Robarts Research Institute, 1151 Richmond Street North, London, Ontario N6A 5B7, Canada. [2]Present address: London Health Sciences Centre, Victoria Hospital, 800 Commissioners Road East, London, Ontario N6G 3G4, Canada. **Address correspondence to:** G.P. e-mail: gparraga@robarts.ca

http://dx.doi.org/10.1016/j.acra.2015.10.010

quantify ventilation abnormalities in patients with asthma. Hallmark MRI findings in these patients include characteristic focal ventilation defects that appear to respond to therapy (7–9) and are related to asthma severity (10–13). In addition, significant changes in ventilation defects are also observed after bronchodilator administration even in the absence of FEV_1 changes, in asthma (14,15) and chronic obstructive pulmonary disease (COPD) (16).

Currently, MRI ventilation abnormalities can be semiautomatically quantified using cluster analysis tools (17–19) that generate ventilation defect percent (VDP), which is the normalized volume of the lung not participating in ventilation. Although the measurements of ventilation defect volumes and percent are very useful, these measurements provide a global lung volume that does not fully exploit the rich information content inherent to ^{3}He ventilation signal intensity textures and patterns that are dictated by the underlying pulmonary pathophysiology.

Second-order texture features in X-ray computed tomography (CT) pulmonary images have been utilized as prognostic biomarkers in patients with nonsmall cell lung cancer undergoing chemotherapy (20) and radiotherapy (21), as well as classifiers of COPD (22), asthma (22), cancer phenotypes (23), and pulmonary fissures (24). ^{3}He MRI ventilation texture tools were also previously piloted in the evaluation of a rodent model of asthma (25) and to differentiate patients with asthma from normal volunteers (26). In addition, the difference in ventilation heterogeneity between healthy subjects and those with asthma was also evaluated using the coefficient of variation of the hyperpolarized ^{3}He MRI signal—a straightforward local texture analysis approach (7).

Based on these previous demonstrations, we hypothesized that second-order texture classifiers could be generated to evaluate ^{3}He ventilation pre- and post-bronchodilator in patients with asthma, providing complementary information to spirometry measurements and VDP and perhaps provide another way to classify bronchodilator response. Therefore, here, our objective was to generate automated second-order texture classifiers of ^{3}He MRI ventilation as biomarkers of bronchodilator response in patients with asthma and compare these to spirometry measurements and VDP.

METHODS

Study Subjects and Pulmonary Function Tests

Participants with a clinical diagnosis of asthma provided written consent to the study protocol approved by a local research ethics board and Health Canada. The study was compliant with the Personal Information Protection and Electronic Documents Act of Canada and the Health Insurance Portability and Accountability Act of the United States.

Pulmonary function tests and imaging were performed before bronchodilator administration using 400 μg of salbutamol (Apo-Salvent Free Inhalation Aerosol; Apotex, Toronto, ON, Canada) and 25–30 min post-salbutamol administration. Salbutamol was delivered through a pressurized metered dose inhaler and AeroChamber Plus valved holding chamber (Trudell Medical International, London, ON, Canada). A body plethysmograph (MedGraphics, Saint Paul, MN) was used for all pulmonary function tests in accordance with the joint ATS-European Respiratory Society guidelines (27).

Asthma Criteria

For safety reasons, we performed Methacholine (MCh) challenge only in patients with baseline $FEV_1 > 65\%$ predicted. Of the 47 patients with asthma evaluated here, 23 were administered MCh challenge and 10 out of 23 patients tested met the criteria for a positive response for MCh hyperresponsiveness (<1 mg/mL (28)). This information was used in the receiver operating characteristic (ROC) analysis as ground truth. Bronchial hyperresponsiveness was evaluated using the provocative concentration of methacholine required for FEV_1 to decrease 20% from baseline (29). Response to bronchodilation was evaluated using ATS guidelines (4) based on a change in FEV_1 of at least 200 mL and/or 12% for FEV_1 responders and a change in VDP of at least 3% for VDP responders.

Image Acquisition

MRI was performed on a whole body 3.0 Tesla Discovery MR750 (GE Health Care, Milwaukee, WI) with broadband imaging capability as previously described (18). ^{1}H MRI was acquired before ^{3}He imaging with a fast spoiled gradient-echo (16 s total data acquisition, relaxation time [TR]/echo time [TE]/flip angle = 4.7 ms/1.2 ms/30°, field of view [FOV] = 40 × 40 cm, matrix 128 × 128, 14 slices, 15 mm slice thickness, 0 cm gap) during a 1 L inspiratory breath-hold of medical grade N_2. For ^{3}He MRI, ventilation images were acquired using a two-dimensional gradient echo sequence (14 s data acquisition, TR/TE/flip angle = 4.3 ms/1.4 ms/7°, FOV = 40 × 40 cm, matrix 128 × 128, 14 slices, 15 mm slice thickness, 0 gap) during inspiratory breath-hold of a 1 L ^{3}He/N_2 (5 mL/^{3}He body weight diluted to 1 L with N_2) mixture.

Image Analysis and Texture Classifier Generation

VDP was generated using a semi-automated segmentation algorithm developed using MATLAB R2013a (The Mathworks Inc., Natick, MA) (18). Subjects were classified as bronchodilator responder based on VDP greater than 3% based on the analysis of ventilation segmentation variability (18).

Figure 1 provides a schematic of the method we used to generate second-order texture features based on the statistical analyses of a gray-level run-length matrix (GLRLM) (30). Briefly, the GLRLM measures texture or the variation of the "gray level" intensity of voxels, quantifying coarseness, and regularity through connected voxels satisfying a given gray-level property that occurs repeatedly in an image region (31). In the current study, MRI ventilation texture features were generated by calculating GLRLMs, and in general, long

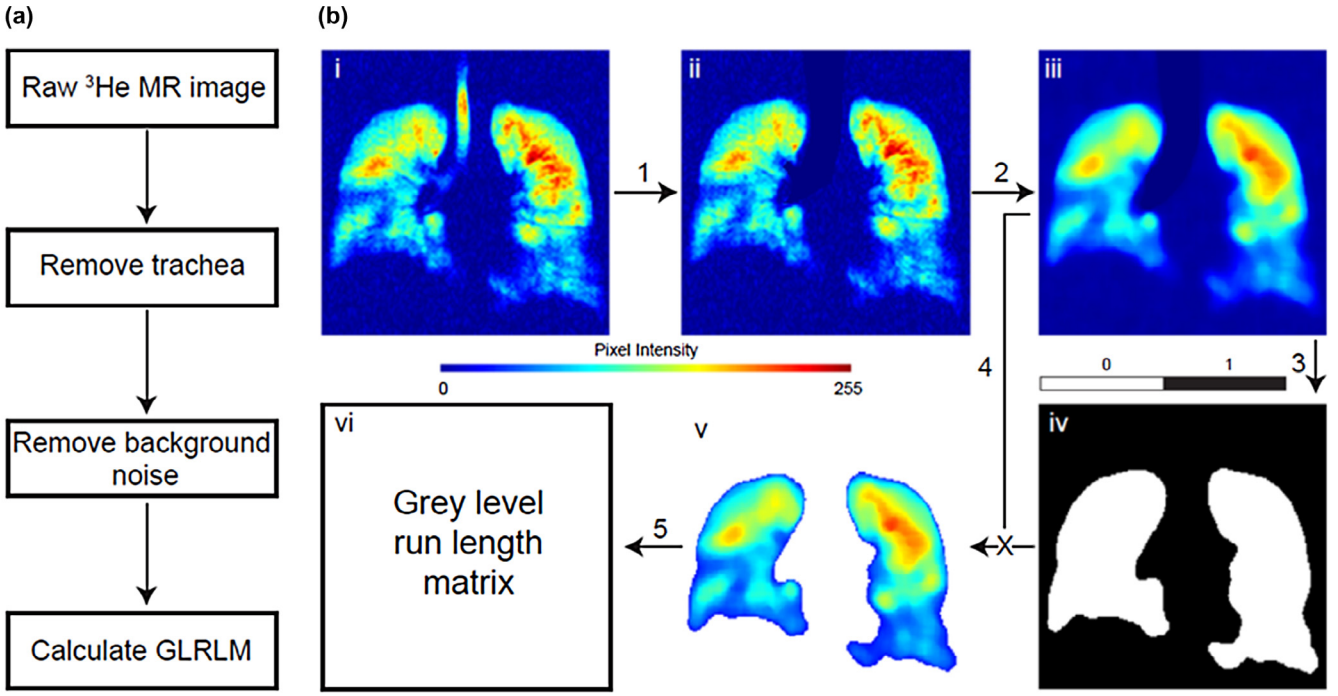

Figure 1. Texture analysis pipeline. **(a)** Pipeline schematic, **(b)** Detailed steps of the pipeline, where i) raw 3He MR image with a colour-map applied to show variations in signal intensity, ii) MR image with trachea removed, iii) filtered MR image used to generate iv) the maximum entropy mask that is multiplied by the filtered MR image to extract the ^{3}He ventilation mask v) used to generate the gray-level run-length matrix (GLRLM) vi) for second-order texture feature calculations. GLRLM, gray-level run-length matrix; MR, magnetic resonance.

gray-level runs correspond to coarse textures, whereas short gray-level runs correspond to finer textures (32).

The signal-to-noise ratio (SNR) was generated for each ^{3}He MRI slice by sampling four 7×7 cm^2 sample voxels of lung parenchyma signal and dividing by the standard deviation of four samples of the background signal as noise. Texture features for each ^{3}He MRI slice with SNR > 15 were averaged. Figure 1a shows the schematic of the texture analysis pipeline, where the raw image was processed before GLRLM was generated. In Figure 1b, a semi-automated algorithm consisting of four steps is described. First, the trachea was removed using manual segmentation. The raw data were then filtered using a 10×10 median filter and then a maximum entropy filter was applied to the filtered image to generate a binary mask with ventilation values = 1 and background values = 0. Finally, the entropy mask was multiplied by the filtered image. This resulted in an image matrix showing only ^{3}He ventilation pixels surrounded by zero-value pixels that were used for the calculation of GLRLM. In this manner, a "ventilation" mask was generated to capture information about changes in ventilation that the calculation of VDP cannot provide. The rationale for focusing on ventilation texture changes stems from our interest in evaluating changes in ventilation patchiness (and not just ventilation defects) in patients with asthma after inhalation of salbutamol and other therapies. The original image contained a high range of intensity values that led to low probabilities of run lengths. Therefore, the image intensities were scaled to 64 values between the minimum and maximum intensities of the image. Neighboring pixels were evaluated in four unique directions: $(i,j) = (0,1)$, $(0, 1/2)$, $(0,-1)$, and $(1,-1/2)$; whereas evaluations in the z-direction were omitted because slice thickness was 15 mm. In this way, GLRLM were generated for each direction, and texture features were averaged.

A total of 11 second-order texture features were generated using Equations 1–11 (30) including: (1) short-run emphasis (SRE), (2) long-run emphasis (LRE), (3) gray-level nonuniformity (GLNU), (4) run-length nonuniformity (RLNU), (5) run percentage (RP), (6) low gray-level run emphasis (LGRE), (7) high gray-level run emphasis (HGRE), (8) short-run, low gray-level emphasis (SRLGE), (9) short-run, high gray-level emphasis (SRHGE), (10) long-run, low gray-level emphasis (LRLGE), and (11) long-run high gray-level emphasis (LRHGE). A run is a sequence of pixels of the same gray-level intensity in a specified direction. Short-run texture features measure the distribution of short runs, which directly correlate to fine textures, whereas the distribution of long runs are measured using long-run texture features and correlates with coarse textures. Low and high gray-level texture features measure the distribution of low and high gray-level intensities respectively. Texture features named using both length and gray-level descriptors measure their joint distribution. Gray-level nonuniformity measures the similarity of gray levels found within an image, where a low value corresponding to gray-level values are similar. RLNU measures the similarity of the length of runs throughout the image, where a high value suggests that the image has varying run lengths. RP measures the distribution of runs in a specific direction and is a measurement of homogeneity.

$$SRE = \frac{1}{n_r}\sum_{i=1}^{M}\sum_{j=1}^{N}\frac{p(i,j)}{j^2} \quad (1)$$

$$LRE = \frac{1}{n_r}\sum_{i=1}^{M}\sum_{j=1}^{N}\frac{p(i,j)}{j^2}\times j^2 \quad (2)$$

$$GLNU = \frac{1}{n_r}\sum_{i=1}^{M}\left(\sum_{j=1}^{N}P(i,j)\right)^2 \quad (3)$$

$$RLNU = \frac{1}{n_r}\sum_{j=1}^{N}\left(\sum_{i=1}^{M}P(i,j)\right)^2 \quad (4)$$

$$RP = \frac{n_r}{P(i,j)\times j} \quad (5)$$

$$LGRE = \frac{1}{n_r}\sum_{i=1}^{M}\sum_{j=1}^{N}\frac{P(i,j)}{i^2} \quad (6)$$

$$HGRE = \frac{1}{n_r}\sum_{i=1}^{M}\sum_{j=1}^{N}P(i,j)\times i^2 \quad (7)$$

$$SRLGE = \frac{1}{n_r}\sum_{i=1}^{M}\sum_{j=1}^{N}\frac{p(i,j)}{i^2\times j^2} \quad (8)$$

$$SRHGE = \frac{1}{n_r}\sum_{i=1}^{M}\sum_{j=1}^{N}\frac{p(i,j)\times i^2}{j^2} \quad (9)$$

$$LRLGE = \frac{1}{n_r}\sum_{i=1}^{M}\sum_{j=1}^{N}\frac{p(i,j)\times j^2}{i^2} \quad (10)$$

$$LRHGE = \frac{1}{n_r}\sum_{i=1}^{M}\sum_{j=1}^{N}p(i,j)\times i^2\times j^2 \quad (11)$$

Statistics

Paired two-tailed *t* tests were used to perform comparisons pre- and post-salbutamol on IBM SPSS Statistics V.23.0 (SPSS Inc., Chicago, IL). The Holm–Bonferroni correction was used to adjust *P* values for all VDP and texture classifier multiple tests. To measure the performance of VDP and texture features as bronchodilator response classifiers, ROC curves were generated using GraphPad Prism V.6.04 (GraphPad Software Inc., San Diego, CA) from which the area under the ROC curve (AUC) was calculated. Methacholine response was used as the truth standard for ROC analysis. Pulmonary function measurements, VDP, texture features, and a VDP–texture composite classifier (calculated using a linear Bayes normal classifier) were evaluated for sensitivity and specificity. Linear regressions and Pearson correlation coefficients were generated using GraphPad Prism.

RESULTS

The demographic characteristics and pulmonary function measurements for 47 participants (18 males, 39 ± 13 yrs) are provided in Table 1. Significant differences between pre- and post-salbutamol measurements were observed for FEV_1 ($P = .0001$), FEV_1/FVC ($P = .0001$), Forced Expiratory Flow at 25 to 75% ($FEF_{25–75\%}$) ($P = .005$), residual volume (RV) ($P = .004$), and RV/total lung capacity (TLC) ($P = .0001$).

TABLE 1. Subject Demographics and Pulmonary Measurements

Parameter	Mean (SD) Pre-Salbutamol ($n = 47$)	Mean (SD) Post-Salbutamol ($n = 47$)	Paired Significance (Two Tailed)
Age (years)	39 (13)	–	–
Male	18	–	–
BMI	30 (11)	–	–
FEV_1 $\%_{pred}$	79 (21)	84 (21)	.0001
FVC $\%_{pred}$	90 (16)	91 (14)	.70
FEV_1/FVC %	71 (13)	74 (13)	.0001
$FEF_{25–75\%}$	48 (26)*	77 (9)[2]	.005†
TLC $\%_{pred}$	100 (14)	97 (12)	.08*
RV $\%_{pred}$	129 (35)	110 (36)	.004*
RV/TLC $\%_{pred}$	128 (26)	114 (25)	.0001*

$\%_{pred}$, percent of predicted value; BMI, body mass index; FEV_1, forced expiratory volume in 1 s; FVC, forced vital capacity; RV, residual volume; SD, standard deviation; TLC, total lung capacity.

* $n = 23$.

† $n = 5$.

Figure 2 shows pre- and post-salbutamol results for six representative participants with regions of improved ventilation identified with *yellow* arrows. As shown in Figure 2, pre- and post-salbutamol ventilation images for three representative bronchodilator responders (S1, S2, S3) were classified according to ATS guidelines (4), and three responders (S4, S5, S6) were classified as VDP responders to salbutamol. VDP responders showed qualitatively improved ventilation post-salbutamol, whereas ATS responders S2 and S3 did not show ventilation improvements. As shown in Figure 3, for representative participant S3, there is qualitative evidence of commonly observed heterogeneous or course-texture findings and homogeneous textures in magnification. In the example for homogenous ventilation, LRE was 2300, LRLGE was 2100, and LRHGE was 4600, which are all quite large values reflective of coarse textures observed in this magnified ventilation sample, whereas for the heterogeneous ventilation example, LRE was 1200, LRLGE was 1100, and LRHGE was 1600, which reflect finer textures magnified in the heterogeneous ventilation sample.

Table 2 provides a summary of mean ventilation defect and texture measurements for all subjects, and for FEV_1- and VDP-responder subgroups before and after salbutamol administration with Holm–Bonferonni-corrected *P* values. There were significant differences pre- and post-salbutamol for VDP ($P = .01$). There were also significant differences for VDP and texture classifiers post-salbutamol in the ATS- ($n = 14$) and

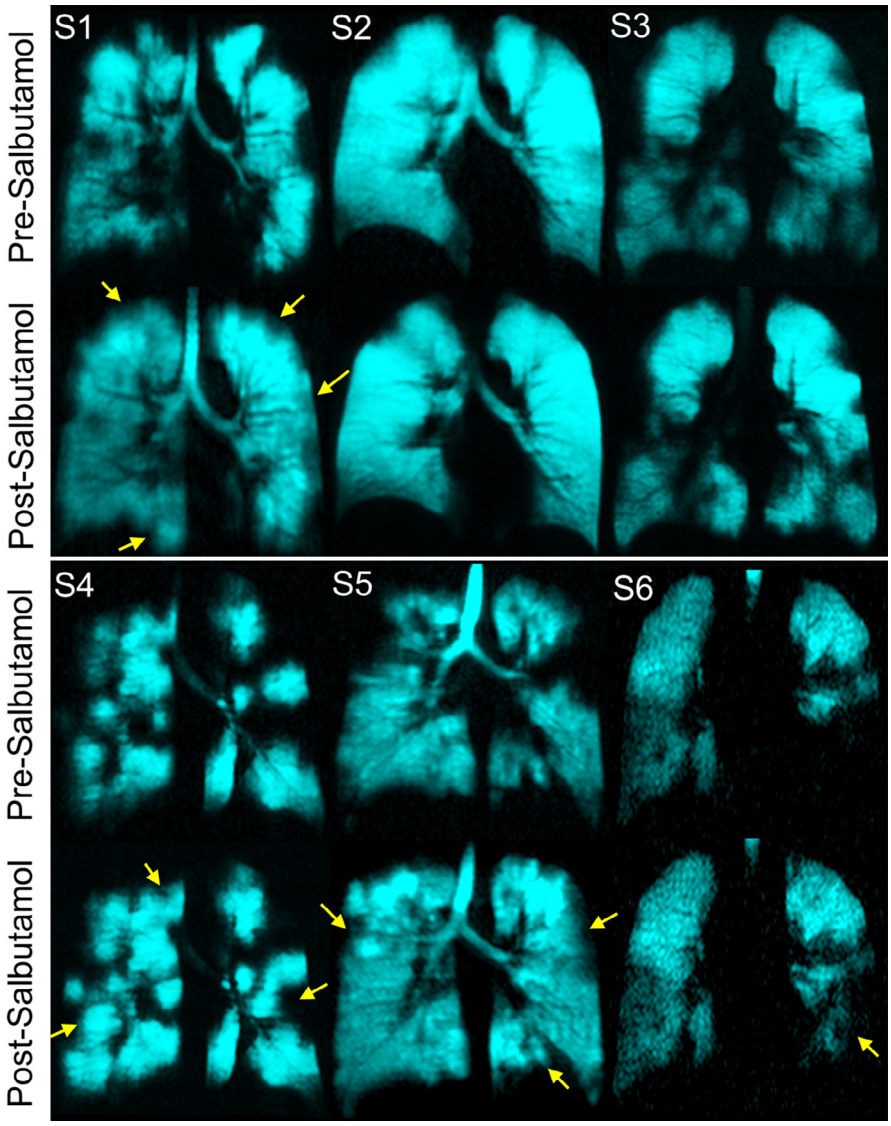

Figure 2. Representative asthma patients with bronchodilator-response measured using ATS criteria and VDP. Subjects S1 to S3 are responders classified according to ATS guidelines while subjects S4 to S6 are VDP-responders. Arrows show ventilation defects that changed post-bronchodilator

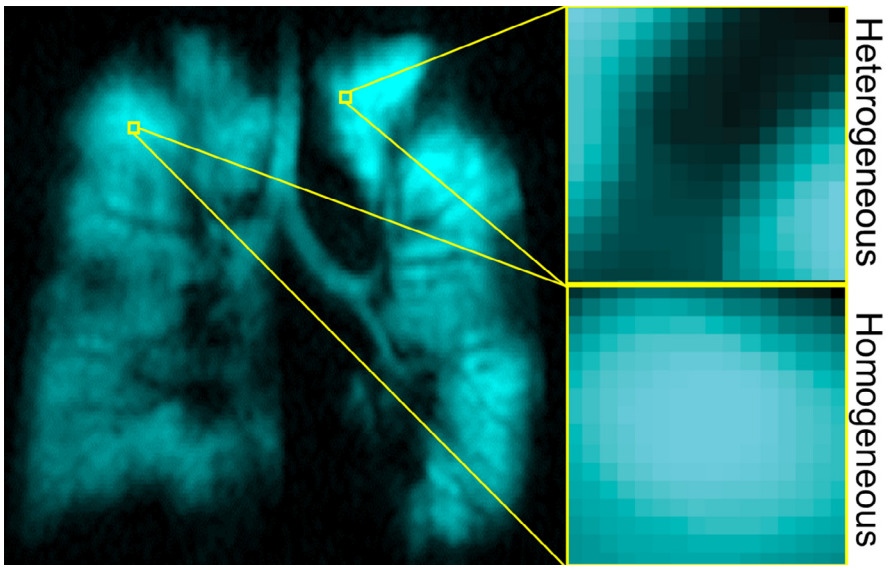

Figure 3. Ventilation and texture measurements. Examples of heterogeneous and homogeneous textures within a ventilation map.

TABLE 2. Ventilation Defect and Texture Measurements

Ventilation Measurements Mean (SD)	All Subjects (n = 47)			Responders (n = 14)			Nonresponders (n = 33)		
	Pre-Salbutamol	Post-Salbutamol	Significance	Pre-Salbutamol	Post-Salbutamol	Significance	Pre-Salbutamol	Post-Salbutamol	Significance
VDP	6 (7)	4 (5)	.01	10 (8)	7 (5)	.07	4 (7)	3 (4)	.5
SRE	.10 (.01)	.10 (.01)	2	.10 (.01)	.10 (.01)	3	.1 (.01)	.1 (.01)	3
LRE	1100 (200)	1100 (100)	2	1000 (150)	1020 (140)	3	1100 (180)	1100 (140)	.6
GLNU	3500 (600)	3400 (700)	.4	3700 (690)	3300 (550)	4	3500 (580)	3400 (700)	2
RLNU	220 (30)	220 (30)	1	220 (25)	220 (34)	2	220 (30)	230 (30)	.8
RP	.40 (.05)	.41 (.05)	.9	.43 (.05)	.41 (.05)	2	.42 (.05)	.41 (.05)	2
LGRE	.70 (.05)	.70 (.05)	.2	.74 (.03)	.72 (.04)	.07	.72 (.03	.72 (.04)	2
HGRE	1400 (320)	1400 (300)	2	1300 (240)	1300 (260)	3	1400 (350)	1400 (300)	3
SRLGE	.002 (.001)	.002 (.001)	.8	.002 (.001)	.002 (.001)	.9	.002 (.001)	.002 (.001)	3
SRHGE	1400 (300)	1400 (300)	2	1300 (240)	1300 (260)	2	1400 (350)	1400 (300)	2
LRLGE	830 (100)	800 (100)	.4	790 (90)	780 (100)	4	840 (110)	810 (80)	.5
LRHGE	6000 (1600)	6300 (1800)	.5	5100 (1500)	6000 (1600)	.04	6400 (1500)	6500 (1800)	1

Ventilation Measurements Mean (SD)	VDP-Derived Responders (n = 10)			VDP-Derived Nonresponders (n = 37)		
	Pre-Salbutamol	Post-Salbutamol	Significance	Pre-Salbutamol	Post-Salbutamol	Significance
VDP	10 (3)	6 (0)	.001	3 (3)	3 (3)	.001
SRE	.1 (.02)	.1 (.01)	3	.1 (.01)	.1 (.01)	.5
LRE	870 (130)	980 (160)	.01	1100 (150)	1100 (130)	.02
GLNU	3700 (800)	3600 (450)	4	3500 (550)	3300 (690)	.2
RLNU	220 (20)	220 (30)	4	220 (30)	220 (30)	1
RP	.42 (.06)	.42 (.05)	.8	.43 (.05)	.41 (.05)	.3
LGRE	.75 (.03)	.71 (.02)	2	.72 (.03)	.71 (.04)	.3
HGRE	1400 (400)	1300 (310)	2	1300 (300)	1400 (290)	2
SRLGE	.002 (.001)	.002 (.001)	2	.002 (.001)	.002 (.001)	2
SRHGE	1400 (400)	1300 (300)	3	1300 (300)	1400 (290)	1
LRLGE	710 (80)	770 (90)	.04	860 (90)	810 (83)	.01
LRHGE	4200 (1000)	5200 (1300)	.1	6500 (1400)	6700 (1700)	.8

GLNU, gray-level nonuniformity; HGRE, high gray-level run emphasis; LGRE, low gray-level run emphasis; LRE, long-run emphasis; LRHGE, long-run high gray-level emphasis; LRLGE, long-run low gray-level emphasis; RLNU, run-length nonuniformity; RP, run percentage; SD, standard deviation; SRE, short-run emphasis; SRHGE, short-run high-level gray emphasis; SRLGE, short-run, low gray-level emphasis; VDP, ventilation defect percent.

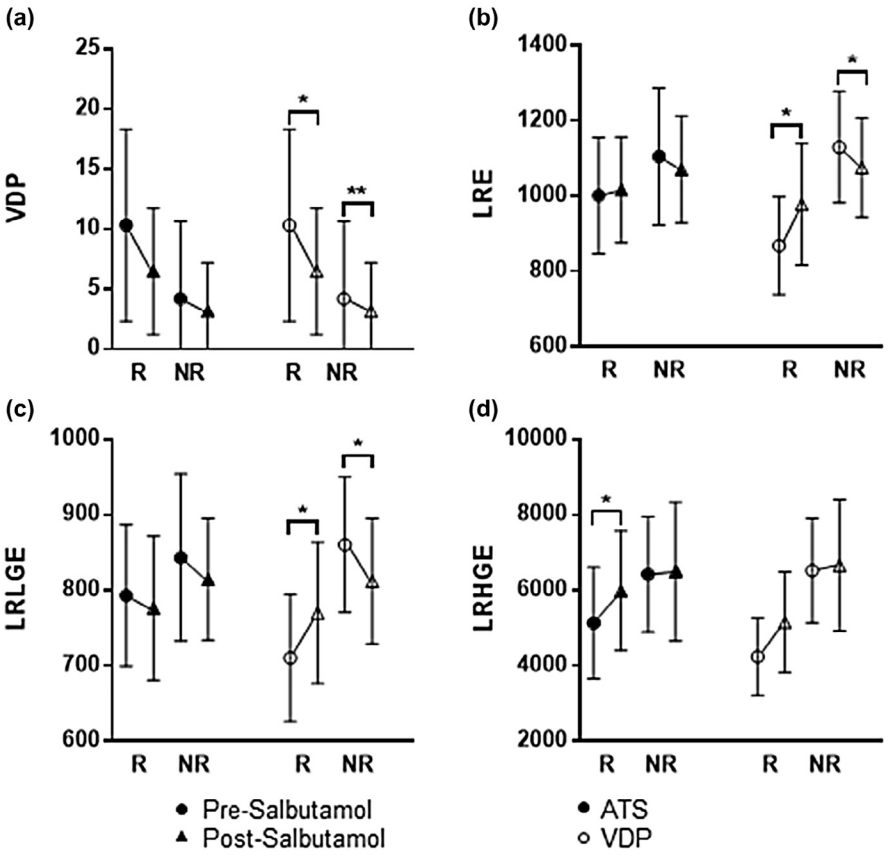

Figure 4. Ventilation defect percent and texture features before and after bronchodilator administration. Significant differences for VDP bronchodilator-responders in LRE (p = .01) and LRLGE (p = .04), and for VDP non-responders in LRE (p = .02) and LRLGE (p = .01). Significant differences were observed for ATS bronchodilator-responders in LHRGE (p = .04). * = p < .05, ** = p < .01 where R = responder, NR = non-responder to bronchodilator administration. ATS, American Thoracic Society; LRE, long-run emphasis LRHGE, long-run, high gray-level emphasis; LRLGE, long-run, low gray-level emphasis; VDP, ventilation defect percent.

VDP-responder ($n = 10$) subgroups. These findings are shown in more detail in Figure 4. For bronchodilator responders based on ATS guidelines using FEV_1, there were significant differences post-salbutamol for the texture feature LRHGE ($P = .04$). For VDP responders, there were significant differences for VDP ($P = .001$), LRE ($P = .01$), and LRLGE ($P = .04$), and for VDP nonresponders there were significant changes for VDP ($P = .001$), LRE ($P = .02$), and LRLGE ($P = .01$).

Figure 5 shows the relationships for coarse-texture features LRE, LRLGE, and LRHGE with VDP and the change in texture features with the change in VDP. Significant correlations were observed for VDP with LRE (R = .5, $P = .0003$), LRLGE (r = .34, $P = .02$), LRHGE (r = .56, $P = .0001$), and percent change in VDP with percent change in LRE (r = .36, $P = .01$) and LRHGE (r = .41, $P = .004$).

In Figure 6, ROC curves show that AUC for VDP (AUC = .92) was significantly greater ($P = 0.001$) than for LRHGE (AUC = .83), FEV_1 (AUC = .80), LRE (AUC = .66), FVC (AUC = .58), and LRLGE (AUC = .42). The LRHGE AUC was significantly greater than LRE ($P = .0001$), FVC ($P = .05$), and LRLGE ($P = .0001$).

DISCUSSION

In this proof-of-concept study, we generated ventilation texture classifiers and used these to evaluate the effects of bronchodilator administration in 47 patients with asthma. We made a number of important observations including: (1) significant differences post-bronchodilator for FEV_1, FEV_1/FVC, RV/TLC, and VDP but not texture classifiers in all patients; (2) significant differences for coarse-texture features LRE and LRLGE for VDP response and VDP nonresponse subgroups, and for LRHGE for the FEV_1–response subgroup; and (3) in ROC curves, VDP (AUC = .92) surpassed FEV_1 (AUC = .80) performance, and LRHGE, a coarse-texture classifier, surpassed FVC, LRE, and LRLGE.

In this study, and as expected based on previous results (10,14,15), there was improved pulmonary function and VDP post-salbutamol in all patients with asthma. These results provide an internal control or check on the post-salbutamol changes in the texture classifiers that were also observed in the VDP-responder and nonresponder subgroups.

Second-order texture analysis of the lung has been previously described in relation to tissue classification for tumor prognosis, segmentation, and lesion diagnosis (20,21,23,24). CT texture features derived from GLRLMs were also shown to be helpful in tissue and organ identification (31). In the current study, MRI ventilation texture features were generated by calculating GLRLMs, and in general, long gray-level runs correspond to coarse textures, whereas short gray-level runs correspond to finer textures (32).

Although there were no texture differences post-salbutamol in all patients, in the VDP-response and nonresponse subgroups, LRE and LRLGE showed significant differences post-salbutamol.

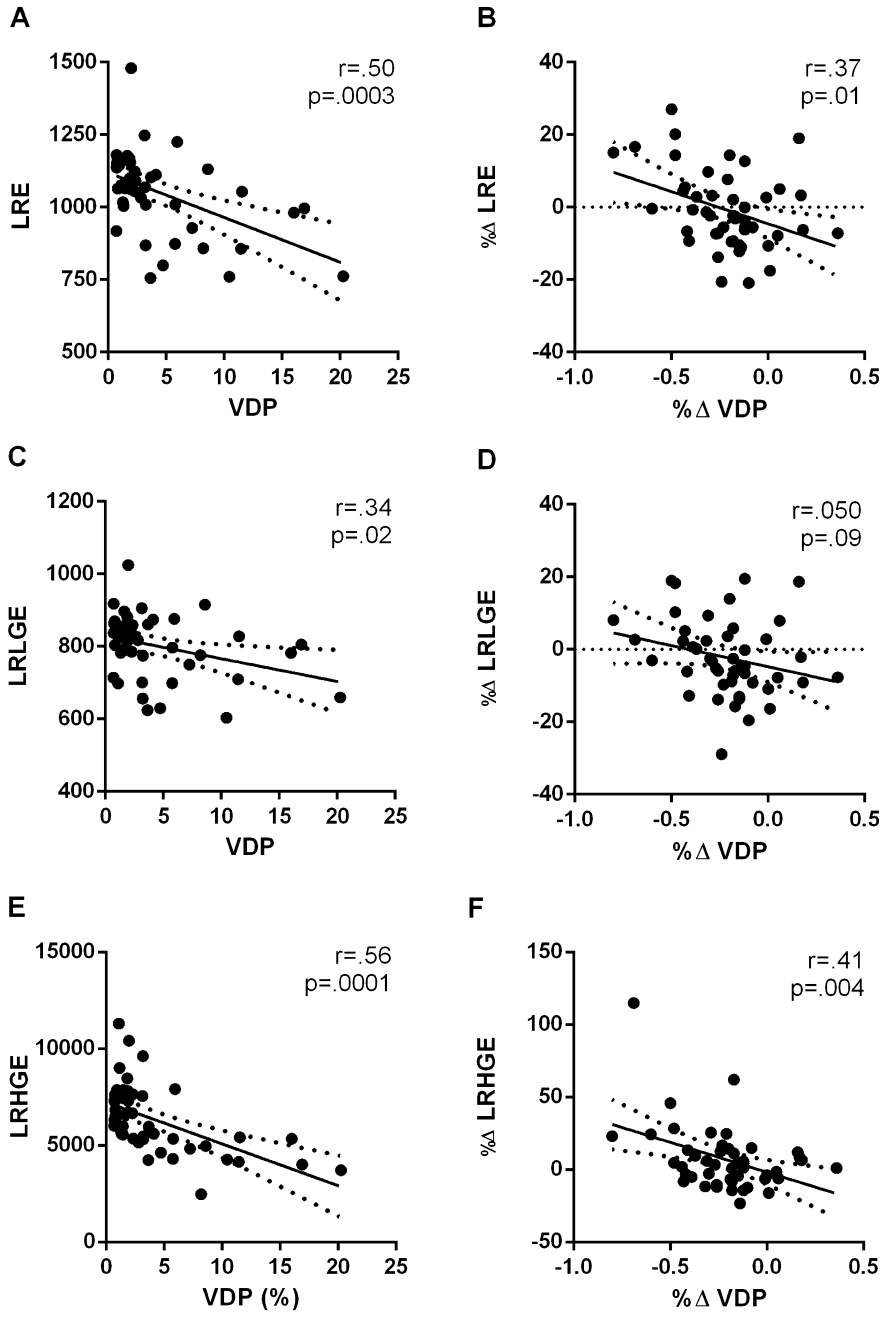

Figure 5. Relationship for ventilation defect percent and texture classifiers. Significant linear regressions for **(a)** VDP with LRE (r = .50, p = .0003), **(b)** percent change in VDP and percent change in LRE (r = .37, p = .01), **(c)** VDP with LRLGE (r = .34, p = .02), **(d)** percent change in VDP and percent change in LRLGE (r = .05, p = not significant), **(e)** VDP with LRHGE (r = .56, p = .0001) and **(f)** percent change in VDP and percent change in LRHGE (r = .41, p = .004). LRE, long-run emphasis LRHGE, long-run, high gray-level emphasis; LRLGE, long-run, low gray-level emphasis; VDP, ventilation defect percent.

In VDP responders, this is certainly an intuitive result, but it also suggests that for VDP nonresponders, there were significant changes in coarse textures that were not reflected by VDP, nor captured using our current segmentation algorithm. This is an important finding that needs to be explored further in other patient groups and perhaps using higher spatial resolution images and ^{129}Xe gas.

It is also important to note that there were no significant differences in the fine texture classifiers for the larger patient group, or for the VDP-responder or nonresponder subgroups. This result was unexpected and suggests that the majority of ventilation differences accompanying bronchodilation were reflected by large-scale functional changes—perhaps reflecting the relatively large voxel sizes ($3 \times 3 \times 15$ mm) acquired using inhaled gas MRI. In addition, the differences observed post-bronchodilation included an increase in LRE and LRLGE in the VDP-responder group, suggesting an increase in coarse textures, reflecting more homogenous and less patchy ventilation. In contrast, in the nonresponder group, there was a decrease in coarse-texture features, suggesting more patchy ventilation in response to salbutamol. This result is consistent with previously published findings of paradoxical response or diminished pulmonary function in some patients with asthma and with COPD post-salbutamol that was also supported in the large COPD gene study (33).

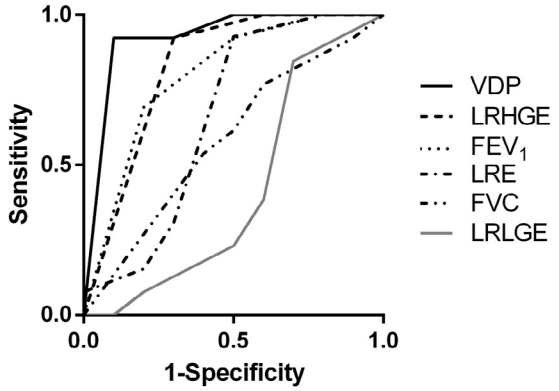

Figure 6. Receiver operator curve for MRI ventilation and pulmonary function measurements. For those 23 patients with asthma with methacholine challenge data: VDP AUC = .92; LRHGE AUC = .83; FEV_1 AUC = .80; LRE AUC = .66; FVC AUC = .58; LRLGE AUC = .42. where FEV_1 is the forced expiratory volume in 1 s. LRE, long-run emphasis; LRHGE, long-run, high gray-level emphasis; LRLGE, long-run, low gray-level emphasis; VDP, ventilation defect percent.

Finally, coarse-texture features were evaluated for their potential to serve as biomarkers of asthma using ROC curves. Although the strongest performance was provided by VDP, the texture feature LRHGE also provided excellent performance that surpassed FEV_1 and all other texture features. Although the sample size is quite small, these preliminary results suggest that both VDP (which is in fact a binary texture measurement) and LRHGE are both sensitive and specific asthma predictors in these patients. That both of these MRI measurements showed greater sensitivity and specificity compared to FEV_1 is an important finding that needs follow-up in studies with a greater number of patients.

We acknowledge a number of study limitations including the relatively small sample size for this proof-of-concept texture classifier evaluation. Certainly, future iterations of this approach will involve a larger and more varied sample size of patients with asthma. We also note that with a larger sample size, we can extend the results reported here in 11 texture classifiers using the leave-one-out method to develop a suite of tools that together can explain differences in post-methacholine challenge in comparison to exercise challenge and to different responses to treatment. Another important limitation is the fact that currently, ventilation defect segmentation is performed semi-automatically and still requires a rigorous training protocol and up to 10 min of processing time/subject image. The texture feature tools we generated here were automated, except for manual trachea removal and the processing time per subject and observer training time is much lower (on the order of 2–3 min per subject image), which a distinct advantage compared to VDP measurements. Given these caveats, the results of this feasibility study should be considered hypothesis generating and point to the need for a larger study in a great number and variety of patients with asthma.

In summary, this study showed that ventilation texture features can be generated from clinical MRI ventilation images and used to quantify lung ventilation differences post-salbutamol. The use of ventilation texture classifiers provides quantitative ventilation patchiness measurements that are complementary to ventilation defect and pulmonary function measurements. We think that ventilation texture features may be used as biomarkers of therapy response in patients with asthma including those responses not detected by pulmonary function tests. Robust, automated, sensitive, and specific biomarkers of asthma lung function are critically needed for better understanding ventilation in the asthmatic lung and for the development of novel asthma treatments.

ACKNOWLEDGMENTS

We gratefully acknowledge funding from a Canadian Institutes of Health Research (CIHR) Team Grant for the Thoracic Imaging Network of Canada, CIHR Operating Grant MOP# 106437. Dr. Parraga also gratefully acknowledges salary support from a CIHR New Investigator award. We thank Sandra Blamires, CCRC, for clinical coordination; Andrew Wheatley, BSc, for production and dispensing of ^{3}He gas; and David Reese, RTMR, for MRI of research volunteers.

REFERENCES

1. Reddel HK, Bateman ED, Becker A, et al. A summary of the new GINA strategy: a roadmap to asthma control. Eur Respir J 2015; 46:622–639.
2. Reddel HK, Hurd SS, FitzGerald JM. World Asthma Day. GINA 2014: a global asthma strategy for a global problem. Int J Tuberc Lung Dis 2014; 18:505–506.
3. National Asthma E, Prevention P. Expert panel report 3 (epr-3): guidelines for the diagnosis and management of asthma—summary report 2007. J Allergy Clin Immunol 2007; 120:S94–S138.
4. Pellegrino R, Viegi G, Brusasco V, et al. Interpretative strategies for lung function tests. Eur Respir J 2005; 26:948–968.
5. Gjevre JA, Hurst TS, Taylor-Gjevre RM, et al. The American Thoracic Society's spirometric criteria alone is inadequate in asthma diagnosis. Can Respir J 2006; 13:433–437.
6. Albert MS, Cates GD, Driehuys B, et al. Biological magnetic resonance imaging using laser-polarized 129XE. Nature 1994; 370:199–201.
7. Tzeng YS, Lutchen K, Albert M. The difference in ventilation heterogeneity between asthmatic and healthy subjects quantified using hyperpolarized ^{3}He MRI. J Appl Physiol 2009; 106:813–822.
8. Kruger SJ, Niles DJ, Dardzinski B, et al. Hyperpolarized helium-3 MRI of exercise-induced bronchoconstriction during challenge and therapy. J Magn Reson Imaging 2014; 39:1230–1237.
9. Thomen RP, Sheshadri A, Quirk JD, et al. Regional ventilation changes in severe asthma after bronchial thermoplasty with (3)HE MR imaging and CT. Radiology 2015; 274:250–259.
10. Altes TA, Powers PL, Knight-Scott J, et al. Hyperpolarized 3HE MR lung ventilation imaging in asthmatics: preliminary findings. J Magn Reson Imaging 2001; 13:378–384.
11. de Lange EE, Altes TA, Patrie JT, et al. Evaluation of asthma with hyperpolarized helium-3 MRI: correlation with clinical severity and spirometry. Chest 2006; 130:1055–1062.
12. de Lange EE, Altes TA, Patrie JT, et al. The variability of regional airflow obstruction within the lungs of patients with asthma: assessment with hyperpolarized helium-3 magnetic resonance imaging. J Allergy Clin Immunol 2007; 119:1072–1078.
13. Svenningsen S, Kirby M, Starr D, et al. What are ventilation defects in asthma? Thorax 2014; 69:63–71.

14. Costella S, Kirby M, Maksym GN, et al. Regional pulmonary response to a methacholine challenge using hyperpolarized (3)HE magnetic resonance imaging. Respirology 2012; 17:1237–1246.
15. Svenningsen S, Kirby M, Starr D, et al. Hyperpolarized (3) HE and (129) XE MRI: differences in asthma before bronchodilation. J Magn Reson Imaging 2013; 38:1521–1530.
16. Kirby M, Mathew L, Heydarian M, et al. Chronic obstructive pulmonary disease: quantification of bronchodilator effects by using hyperpolarized (3)He MRI imaging. Radiology 2011; 261:283–292.
17. Tustison NJ, Avants BB, Flors L, et al. Ventilation-based segmentation of the lungs using hyperpolarized (3)He MRI. J Magn Reson Imaging 2011; 34:831–841.
18. Kirby M, Heydarian M, Svenningsen S, et al. Hyperpolarized 3He magnetic resonance functional imaging semiautomated segmentation. Acad Radiol 2012; 19:141–152.
19. He M, Kaushik SS, Robertson SH, et al. Extending semiautomatic ventilation defect analysis for hyperpolarized (129)XE ventilation MRI. Acad Radiol 2014; 21:1530–1541.
20. Ahn SY, Park CM, Park SJ, et al. Prognostic value of computed tomography texture features in non-small cell lung cancers treated with definitive concomitant chemoradiotherapy. Invest Radiol 2015; 50:719–725.
21. Mattonen SA, Palma DA, Haasbeek CJ, et al. Early prediction of tumor recurrence based on ct texture changes after stereotactic ablative radiotherapy (SABR) for lung cancer. Med Phys 2014; 41:033502.
22. Meier A, Farrow C, Harris BE, et al. Application of texture analysis to ventilation SPECT/CT data. Comput Med Imaging Graph 2011; 35:438–450.
23. Gao M, Fan T, Duan J. SU-E-E-16: the application of texture analysis for differentiation of central cancer from atelectasis. Med Phys 2015; 42:3226.
24. Wei Q, Hu Y. A study on using texture analysis methods for identifying lobar fissure regions in isotropic CT images. IEEE Eng Med Biol 2009; 3537–3540.
25. Risse F, Pesic J, Young S, et al. A texture analysis approach to quantify ventilation changes in hyperpolarised (3)He MRI of the rat lung in an asthma model. NMR Biomed 2012; 25:131–141.
26. Tustison NJ, Altes TA, Song G, et al. Feature analysis of hyperpolarized helium-3 pulmonary MRI: a study of asthmatics versus nonasthmatics. Magn Reson Med 2010; 63:1448–1455.
27. Miller MR, Hankinson J, Brusasco V, et al. Standardisation of spirometry. Eur Respir J 2005; 26:319–338.
28. Cockcroft DW. Direct challenge tests: airway hyperresponsiveness in asthma: its measurement and clinical significance. Chest 2010; 138:18S–24S.
29. Mauger EA, Mauger DT, Fish JE, et al. Summarizing methacholine challenges in clinical research. Control Clin Trials 2001; 22:244S–251S.
30. Tang X. Texture information in run-length matrices. IEEE Trans Image Process 1998; 7:1602–1609.
31. Ergen B, Baykara M. Texture based feature extraction methods for content based medical image retrieval systems. Biomed Mater Eng 2014; 24:3055–3062.
32. Galloway MM. Texture analysis using gray level run lengths. Comput Graph Image Process 1975; 4:172–179.
33. Bhatt SP, Wells JM, Kim V, et al. Radiological correlates and clinical implications of the paradoxical lung function response to beta(2) agonists: an observational study. Lancet Respir Med 2014; 2:911–918.